

CloSE: A Compact Shape- and Orientation-Agnostic Cloth State Representation

Jay Kamat, Júlia Borràs, Carme Torras

Abstract— Cloth manipulation is a difficult problem mainly because of the non-rigid nature of cloth, which makes a good representation of deformation essential. We present a new representation for the deformation-state of clothes. First, we propose the *dGLI disk representation*, based on topological indices computed for segments on the edges of the cloth mesh border that are arranged on a circular grid. The heat-map of the dGLI disk uncovers patterns that correspond to features of the cloth state that are consistent for different shapes, sizes of positions of the cloth, like the corners and the fold locations. We then abstract these important features from the dGLI disk into a circle, calling it the *Cloth StatE representation* (CloSE). This representation is compact, continuous, and general for different shapes. Finally, we show the strengths of this representation in two relevant applications: semantic labeling and high- and low-level planning. The code, the dataset and the video can be accessed from : <https://jaykamat99.github.io/close-representation/>

I. INTRODUCTION

Cloth manipulation is a challenging problem in robotics mainly because of the cloth infinite-dimensional configuration space, i.e. the space of possible cloth positions (or states) in space. Unlike rigid or even articulated objects, where one just needs the object pose and joint configurations in case of articulations, clothes can deform in multiple ways making it extremely difficult to have a simplified representation. In addition, the various shapes, sizes, and mechanical properties of clothes add to the difficulty. For this reason, end-to-end learning-based methods struggle to learn to manipulate clothes even in simulation, because by sampling examples it is nearly impossible to explore all the configuration space. In addition, perception is misleading because these objects have a lot of self-occlusions and intricate shapes even in simulated images. Several reviews in literature point to the need of a simplified good representations that could pave the way for having more efficient learning methods [1–3].

In recent years, many datasets with both real and simulated clothes have emerged, as summarized in [4]. Real images lack ground truth information on the configuration of cloth, and many reconstruction works [5, 6] rely on realistic simulated images where the ground truth is the full mesh. But even then, there is no real understanding of the configuration of cloth other than comparing to predefined

The research has been partially supported by project PID2023-152259OB-I00 (CHLOE-MAP), MCIU/ AEI /10.13039/501100011033, project ROBassist (CSIC code 202450E060), and by ERDF, UE and project SoftEnable (HORIZON-CL4-2021-DIGITAL-EMERGING-01-101070600)

All authors are with the Institut de Robòtica i Informàtica Industrial, CSIC-UPC

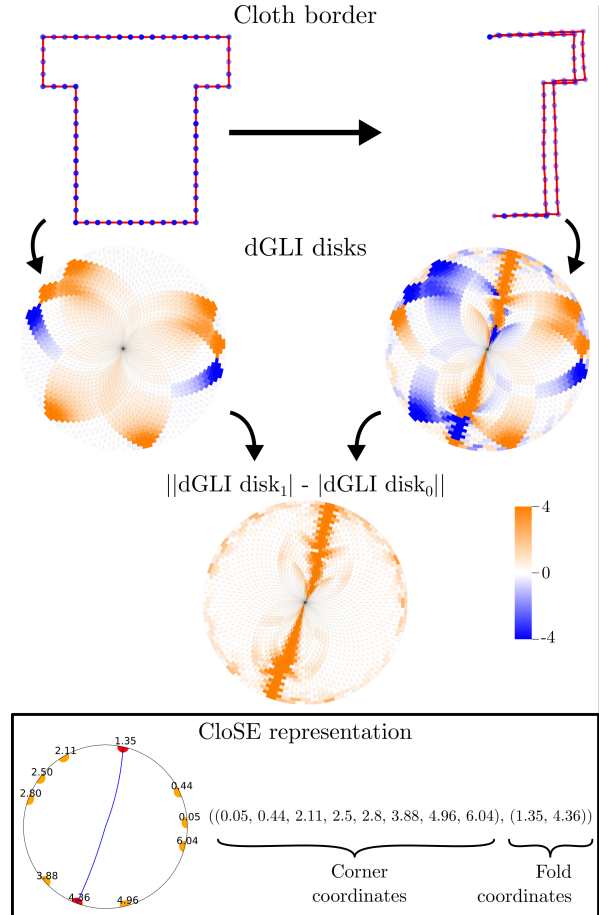


Fig. 1: Example of CloSE derivation: From the border, we compute the dGLI disk where each petal corresponds to a corner. The difference between dGLI disks for the start and end frames allows to extract the fold information, so as to obtain the final CloSE descriptor that is shown graphically and numerically at the bottom of the figure.

states or recognizing which pixels are sleeves or collars. In other words, there is no definitive solution to reason on the configuration space of cloth. In addition, partial solutions are costly and inefficient because robots could work with much less information than the full mesh. For instance, previous works have shown how recognizing salient features, corners or borders is enough for effective manipulation [7, 8]. Existing solutions to navigate the configuration space of cloth are based on RGB-D zenithal images of folded states [9, 10], that effectively learn observed transitions between the

silhouette of observed states.

Authors in [11] mathematically prove how for developable surfaces, as cloth is if assumed to be inextensible, the border pose defines the configuration of the entire cloth. This inspired works such as [12] where topological indices were measured on the border of the cloth to characterize its state. In particular, they applied a derivative of the Gauss Linking Integral (GLI), an index that measures the linking number of curves, to the border of cloth to define a representation that allowed to cluster different cloth states just using a distance. Our paper takes inspiration from this work, but goes beyond by representing the GLI derivative matrix in a novel way that allows to define a very compact representation of the folding state of cloth, the CloSE representation, that is independent of the shape of the silhouette of the unfolded flat state, continuous and fully analytical, and allows to reconstruct cloth state from it.

Our CloSE representation encodes:

- The shape of the cloth, i.e., the location of the corners of the silhouette of the flat unfolded state of the cloth
- The location of the folds and their orientations (which side folds up)

We propose a method departing from the work of [12], taking all edges along the border and calculating the dGLI. The first important novelty is that we arrange these values in a circular grid instead of a matrix, and we call it the dGLI disk. We then use simple clustering and curve fitting algorithms to get the coordinates for our proposed representation. Fig. 1 shows the starting and final cloth borders of a folding action, their corresponding dGLI disks, the subtraction operation that allows to define the fold coordinates, and the CloSE representation obtained after our curve fitting. It is worth noting that the dGLI disk encodes other cloth-state characteristics in addition to first folds, like multiple folds or wrinkles, which could be added to the CloSE descriptor and will be studied in future works.

The contributions of this paper include

- 1) A new dGLI representation arranged in a disk instead of a matrix, which unravels a hidden structure.
- 2) A novel very compact representation, CloSE, that generalizes to any shape and pose of the cloth, as well as the code to derive it given the cloth border.
- 3) Two applications of the CloSE representation: defining an automatic semantic description of the cloth state and planning manipulation sequences.

II. RELATED WORK

The configuration space of cloth is the space of possible cloth states in the Euclidean space. Different representations have been used in literature for robotic manipulation applications. Ranging from the full mesh of a simulated cloth [13] to simplified geometric representations of the silhouettes [14–16], none of these representations permit reasoning in this space in a general way, as they are highly dependent on the cloth shape. Later learning approaches relied on directly using the RGB or RGB-D as representation of the state of cloth

[17–19], usually limited to zenithal views but still allowing to encode folding states. One example is [9], where a lower dimensional latent space of different observed states was encoded as a road-map to plan actions. Since these works map directly from the RGB image space to the latent space without any knowledge of the cloth (implicit or explicit), the latent space representation is not continuous, that is, the intermediate steps cannot be visualized. In addition, these data-based methods require a lot of training data for each cloth shape. Our proposed representation assumes a given border curve, but from that, it is general for any shape.

The idea of using the Gauss Linking Integral (GLI) for robotics applications is not new. The GLI has been applied to representative curves of the workspace to guide path planning through holes [20, 21], for guiding caging grasps in [22–24], and for planning humanoid robot motions using the GLI to guide reinforcement learning [25]. The idea of applying the GLI to the curve that represents the border of the cloth was used in [12]. For planar curves the GLI is degenerated and clothes on a table are mostly planar, therefore, [12] proposed to apply a directional derivative of the GLI, leading to the dGLI coordinates, which enable distance reasoning in the C-space of cloth. This representation was used in [26] to learn semantic tags of a dataset of folding states of a squared piece of cloth. The dGLI coordinates rely on choosing a few segments in the border to calculate the dGLI, and this makes them sensitive to changes in the chosen segments and may not be indicative of how the cloth behaves as a whole. Our work mitigates this by choosing all edge segments for the dGLI calculation instead of a few. This choice does increase the dimension of the dGLI coordinates, but they are only used to derive the CloSE representation, that is of much lower dimension.

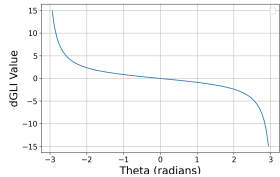
Our proposed method requires to know the curve of the border of the silhouette, which is a limitation. For simulated clothes this can be obtained because we have the full mesh. For perception of real cloth, there are several works that already are able to identify either the mesh of the cloth [27] or directly identify the border [8, 28], and therefore, they open the door to calculate our representation from real cloth images.

To the best of our knowledge, this is the first time a continuous representation of the folding state of cloth is proposed that is independent of the cloth shape, continuous and enables the reconstruction of the state of cloth given the initial unfolded state. This representation is general, but in this work we will only present results for one fold, although in future work we are already working on the generalization of the representation to multiple folds.

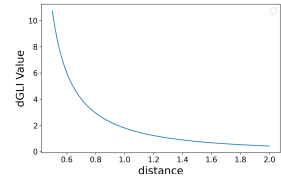
III. BACKGROUND - dGLI

The Gauss Linking Integral (GLI) Eq.1 measures the linking number between two closed curves.

$$G(\gamma_1, \gamma_2) = \frac{1}{4\pi} \int \int \frac{(\gamma_2 - \gamma_1) \cdot [\gamma'_2 \times \gamma'_1]}{\|\gamma_2 - \gamma_1\|^3} \quad (1)$$



(a) Variation of dGLI with angle between segments



(b) Variation of dGLI with distance between segments

Fig. 2: Behavior of dGLI in case of planar segments

The work in [29] shows that the Linking Integral computed between two open curves can also be used for many real world applications because it measures how much the two curves revolve around each other. They introduced a discrete version of the formula above based on the computation of the GLI between the segments that form the curves. The GLI between two line segments can be calculated as

$$\begin{aligned} \mathcal{G}(\gamma_{AB}, \gamma_{CD}) &= \arcsin(\vec{n}_a \cdot \vec{n}_b) + \arcsin(\vec{n}_b \cdot \vec{n}_c) \\ &\quad + \arcsin(\vec{n}_c \cdot \vec{n}_d) + \arcsin(\vec{n}_d \cdot \vec{n}_a) \end{aligned} \quad (2)$$

$$\begin{aligned} \vec{n}_a &= \frac{\vec{AC} \times \vec{AD}}{\|\vec{AC} \times \vec{AD}\|}, \quad \vec{n}_b = \frac{\vec{BC} \times \vec{BD}}{\|\vec{BC} \times \vec{BD}\|}, \\ \vec{n}_c &= \frac{\vec{CD} \times \vec{CA}}{\|\vec{CD} \times \vec{CA}\|}, \quad \vec{n}_d = \frac{\vec{DA} \times \vec{DB}}{\|\vec{DA} \times \vec{DB}\|} \end{aligned}$$

Since the measure GLI vanishes when the segments are coplanar the work in [12] introduced the directional derivative of the GLI along the zenithal axis, called the dGLI.

$$\text{dGLI}(\gamma_{AB}, \gamma_{CD}) = \frac{\mathcal{G}(\gamma_{AB+\epsilon}, \gamma_{CD+\epsilon}) - \mathcal{G}(\gamma_{AB}, \gamma_{CD})}{\epsilon} \quad (3)$$

where ϵ is a small perturbation in the zenithal direction of the cloth made only to points B and D .¹ In [12] the *dGLI coordinates* were defined as all the crossed computations of the dGLI for a few of the segments of the border of the cloth.

The dGLI coordinates can be also arranged as a matrix, whose heat-map show interesting different patterns depending on the cloth state. To understand them, we study how the value of the dGLI for two segments behaves. We have numerically evaluated the dGLI for planar segments for continuously varying angle with constant distance. The resulting graphs are shown in Fig. 2a. Notice that dGLI is 0 when the lines are co-linear, positive on one side and negative on the other. The value of dGLI also decreases as the distance between the 2 segments increases, as shown in Fig. 2b.

IV. REPRESENTATION

We propose two novel cloth representations. The first is the **dGLI disk**, which is inspired by [12], and the second is

¹For calculating dGLI, in this paper we use $\text{dGLI} = \frac{\mathcal{G}(x+2\epsilon) - \mathcal{G}(x+\epsilon)}{\epsilon}$. This does not change any of our analysis. We do this to handle consecutive edge segments.

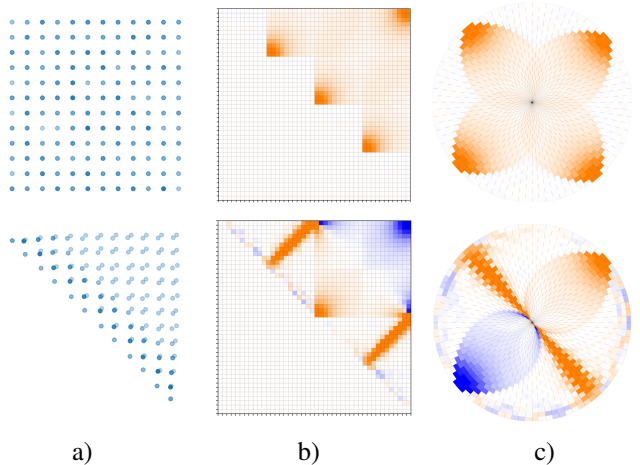


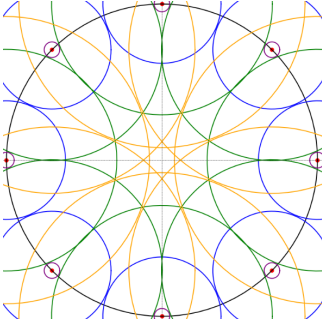
Fig. 3: a) A square napkin mesh. b) The corresponding original dGLI matrix as in [12] and c) Our proposed arrangement in the dGLI disk

the compact and continuous representation that we get from the dGLI disk, the **CloSE** representation.

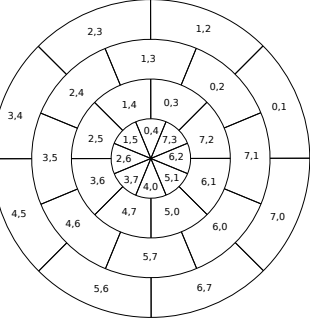
A. The dGLI disk

The dGLI disk is a novel circular arrangement for the dGLI between edges on the border of the cloth. To understand this, we will take the example of a square napkin folded diagonally as shown in Fig. 3. Unlike in [12], where the authors used only a few edges in the dGLI matrix representation, we use all the edges on the border of the mesh. This is done to also capture more information about the cloth. Calculating the dGLI's between all edges and placing them in the semi-matrix form as in [12] gives us a grid as shown in Fig. 3-b, where the heatmap of the matrix is shown, with white colors representing zero values, and orange colors indicating positives and blues negatives. In this form we can already see interesting patterns but they are difficult to interpret. Noticing that information about the corners is present in some sense on the diagonal and the top-right corner, we propose a new arrangement of this semi-matrix on a circular grid such that the grid cells on the diagonal and the corner are now on the border of this disk and all other cells are arranged inside.

To achieve this, we propose a new mapping as shown in Fig. 4b. Here, the dGLI between the neighboring edges is mapped onto the outermost (first) layer. The dGLI between the second neighbor edges is mapped onto the second layer. As for the location of the grid cells, we first symmetrically mark E points on the border of our disk, where E is the number of edges on the border of the mesh. We propose to place $dGLI(i, j)$ at a position somewhat close to the midpoint of an imaginary line joining points i and j marked on the disk border. This is the point where circles of equal radii drawn from i and j would just touch. We notice from Fig. 4a that this form a masonry brick structure as shown in Fig. 4b. Notice that there are $\lfloor E/2 \rfloor$ layers and every layer has exactly E elements. For the last layer, if E is even, we



(a) The intersecting circles



(b) The dGLI mapping

Layer-wise arrangement of grid cells.	
$\{dGLI(i, j) \mid mod(i - j) = 1\}$	layer 1
$\{dGLI(i, j) \mid mod(i - j) = 2\}$	layer 2
$\{dGLI(i, j) \mid mod(i - j) = 3\}$	layer 3
$\{dGLI(i, j) \mid mod(i - j) = 4\}$	layer 4
:	:

Fig. 4: The proposed dGLI disk mapping of the values of $dGLI(i, j)$

have only $E/2$ unique elements, in which case we map the two opposite cells in the last layer to the same value (see Fig. 4b).

This new arrangement allows for much easier interpretation as clear geometric shapes appear, as in the example shown in Fig. 3-c. In the dGLI disk we see a bright flower pattern in the unfolded configuration indicating 4 corners. The representation for the folded cloth adds an orange line between the two folded corners passing through the center, and the petals corresponding to the folded corners change colors. These patterns are consistent across all shapes.

The pattern of the corners holds true by construction because dGLI values are higher when the edges are near and at an angle, as shown in the graphics in Fig. 2, and appear as positive or negative depending on their relative orientation, and when folded, they change sign. Also, when the cloth folds, edges on the opposite sides of the fold come closer resulting in the fold curve. All fold curves on our dGLI disk are straight for a half-fold and curves for other folds, and they always pass through the center. Note that the features depending on the shape of the border, like the corners, appear in the disk with the same values, changing their sign, for all the folding states. That is, the petals of the corners are constant through all the states of the cloth. More examples of the dGLI disk can be seen in the website and the video.

The dGLI disk shows many other features that depend on the cloth state, but in this work we have focused on single folds. In the next section we will see how by applying simple methods to the dGLI disk image we can identify the features to form a very compact representation that we called CloSE.

B. The Cloth StateE (CloSE) representation

The CloSE representation is a compact, continuous representation for cloth folding that keeps track of the corner and

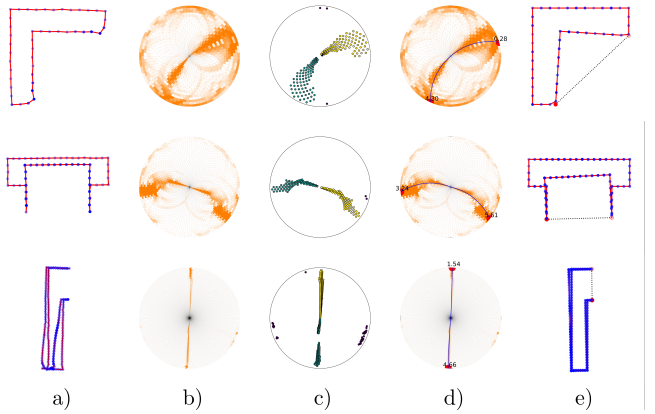


Fig. 5: Column a) shows the border of the cloth mesh, b) the dGLI disk difference, c) the clustered selected points from the dGLI disk difference, d) shows the resulting fitted curve and the computed fold coordinates, printed over the dGLI disk difference, and e) shows the reconstructed mesh from the initial cloth border using the CloSE representation.

the edges.

We define a list of vectors, where the first vector stores the corner locations in radians, i.e., its location on the dGLI disk. Similarly we store the fold locations as subsequent vectors where the two end points of the fold (in radians) denote the location of the fold. The order of these points also denotes the orientation of the fold. That is, a fold (f_1, f_2) will imply that the corners on the route from f_1 to f_2 in the anticlockwise sense will be folded. (see Fig. 1). This notation ensures that all values of (f_1, f_2) are valid folds, hence, we can continuously linearly interpolate from one folded state to another. Some examples are shown in the accompanying video.

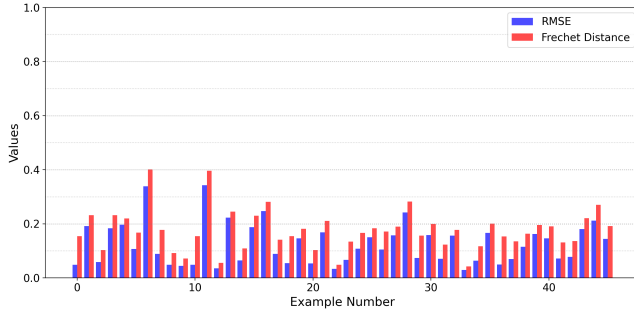
1) *Computation of the corner coordinates v_1, \dots, v_n :* To get the corners we simply iterate through the first layer in the dGLI disk and note the location of the points that are above a certain threshold. Since the first layer only contains dGLI between immediate neighbors, one corner will only give one bright cell. This algorithm though naive did prove to be robust to noise. Coordinates are one-dimensional as they are represented only by the angle in radians inside the disk.

2) *Computation of the fold coordinates (f_1, f_2) :* This problem is a little bit more involved as we need to detect if there is a curve through the center and fit a curve through it. The points where this fitted curve intersects the border of the disk determines the location of the folds.

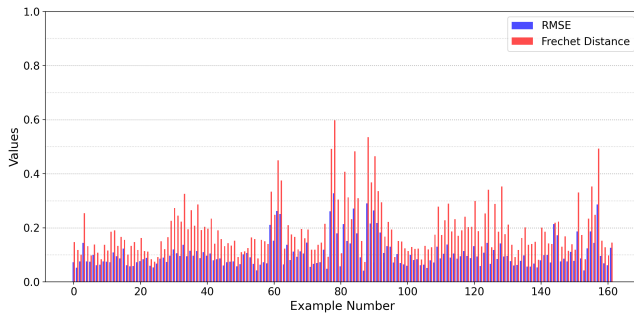
In order to observe the folding pattern more clearly, we take the difference between the initial and final dGLI disks as

$$dGLI \text{ Disk}_{\text{diff}} = ||dGLI \text{ Disk}_{\text{end}} - dGLI \text{ Disk}_{\text{start}}||. \quad (4)$$

This isolates the changes occurred on the cloth due to the folds, because the petals patterns depending on the corners are constant through out all the manipulation, only changing sign. Several examples can be seen in Fig. 5-b.



(a) The MATLAB dataset



(b) The VR dataset

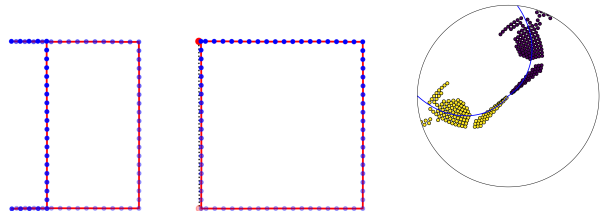
Fig. 6: Error of the comparison between the reconstructed borders of folded clothes from the CloSE representations and real end-frames of the folded clothes

We use this dGLI $Disk_{diff}$ to determine if the cloth has been folded and also to locate the fold on the cloth. To this end, we first get the (polar) coordinates of the cells above a certain threshold and cluster them using the DBSCAN [30]. The clustering algorithm uses a custom metric for circular distances defined as

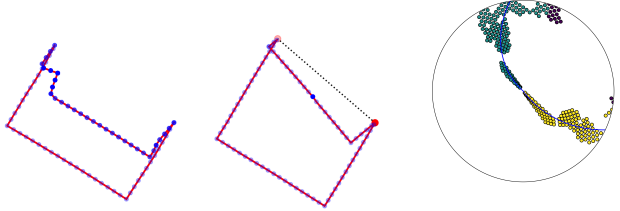
$$d(x_1, x_2) = \sqrt{(\theta_1 - \theta_2)^2 + (r_1 - r_2)^2}, \quad (5)$$

and a minimum sample size. This ensures that points near the center that may be close in the Euclidean sense are clubbed into different clusters, which is useful when there is more than one fold. To detect a single fold, there have to be two clusters corresponding to curves from a point on the border to the center. If the algorithms finds only 1 or more than 2 clusters, it is considered it fails to detect the fold. Example results of the clustering are shown in Fig. 5-c. For each cluster found, we then fit a curve $\theta = p(r)$, where $p(\cdot)$ is a polynomial function in the polar coordinates (θ, r) . We found polynomials of degree 1 to work the best for all examples. Note that in polar coordinates, polynomials of degree 1 are curves. Examples of the resulting fitted curves are shown in Fig. 5d.

3) Ordering of (f_1, f_2) to encode the fold orientation: Corners affected by the fold, change sign, hence, it is easy to detect them. In addition, we order the fold coordinates (f_1, f_2) such that the folded corners lie between f_1 to f_2 while traversing in the anti-clockwise sense. That means that sometimes $f_2 < f_1$.



(a) Example #78 on the VR dataset



(b) Example #157 on the VR dataset

Fig. 7: Some examples of the ground truth border and the reconstructed ones that give the highest errors

TABLE I: Percentage of examples for which a fold is detected by the clustering algorithm

Dataset	min_samples	fold detection success
MATLAB	$E/4$	94.1%
VR	$E/2$	95.9%

V. EVALUATIONS

We evaluate our method of getting the CloSE representation on 2 datasets:

- 1) A dataset we generated on MATLAB using the cloth simulator presented in [31]
- 2) The dataset from [26] up to one fold.

Both the datasets contain the start and the end configuration of folding sequences. The MATLAB dataset contains different shapes (Napkins with varied dimensions, T-shirts with varied dimensions, pants and a circular towel), while the dataset from [26], hereon referred to as the VR dataset, only contains square napkins. The VR dataset is generated by tracking human actions on the cloth in a virtual environment, thereby being more realistic and has a less accurate mesh and more noise. This dataset also contains $\approx 40\%$ examples where the cloth is placed at varied location and orientation.

Using the start and the end configuration from these datasets, we evaluate the success of the method described in Section IV-B for estimating the CloSE representation, that is, the one that correctly detects the number of corners and the location of the folds. As mentioned in the previous section, to detect the folds we first choose the high value points from the dGLI $Disk_{diff}$ depending on a threshold σ . This threshold is defined as the standard deviation of all the values in dGLI $Disk_{diff}$. We then cluster these points using the DBSCAN clustering with $\epsilon = 0.3$. We found that different min sample sizes work well for the two datasets. For the MATLAB dataset we use min_samples as $E/4$ while for the VR dataset we use min_samples as $E/2$. As we know that

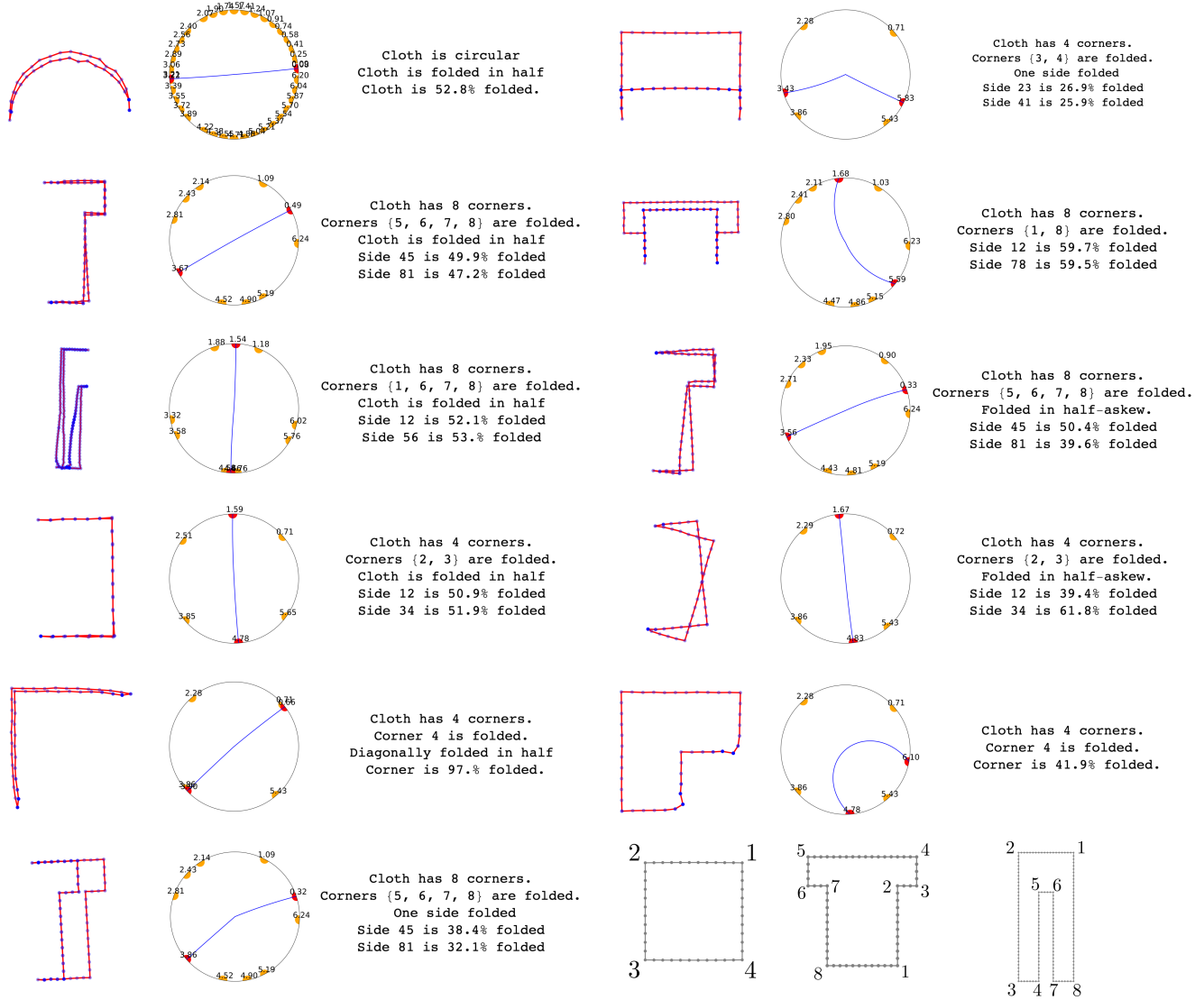


Fig. 8: Different examples of the CloSE representation and the corresponding automatic generated label.

all our dataset elements have folds, if our methods doesn't find any fold we count it as a fail. Table.I shows the success rate of the fold finding algorithm.

Our CloSE representation has enough information to reconstruct the border of the final state given the first one, by actually performing the flip of the border mesh at the indicated fold locations of the detected folded corners. Examples of reconstructed final meshes are shown in Fig. 5-e). We measure how well the representation works by comparing the reconstructed border with the real final border, that is taken as ground truth. We compare the two borders by calculating the Root Mean Squared Error (RMSE) and the Frechet distance between the two curves. The results are shown in a histogram Fig. 6. For fair comparison between different shapes, all examples are scaled to exactly fit into a unit circle with the centroid of the border being the center of the circle.

A. Analysis of the evaluation

We see that our naive method works well on most of the examples, however, it fails to detect the fold in about 5% of the cases. These errors arise because sometimes the classifier detects only one cluster when in reality 2 exist or mis-classifies concentrated noise as a 3rd cluster. In the future we will improve this method to avoid this kind of error.

Once a fold has been detected, we see in Fig. 6 that the distance between curves is around 0.1 for most of the cases (mean = 0.105(rmse)), meaning the representation is accurate enough to do an almost perfect reconstruction. There are some cases, however, where the error is higher. These cases sometimes arise when the cloth is folded close to the border (Fig. 7a) or because of noise or other features, not yet studied on the dGLI disk (Fig. 7b). In either of these cases, the best-fit curve gets pulled away predicting a slightly different fold. When a cloth side is folded, the fold curve changes

direction twice. When the fold is very small the change of direction happens very close to the border, which our defined best-fit-curve fails to accurately capture. Note that this is not a drawback of the CloSE representation but of the detection method. Future work will be directed towards building a better estimator that handles these cases. Having discussed the worse cases, it is important to point out that our method works almost flawlessly for most examples. Many more examples are displayed on our website.

We want to point out that a comparison with any learning approach to recognize fold states would require a lot of training data for each one of the possible folds to identify and for each one of the fold shapes to reach a similar success rate.

VI. APPLICATIONS

We present two applications that arise naturally from our CloSE representation: automatic semantic labeling and high- and low-level planning.

A. Semantic Labeling

Given the CloSE representation of a cloth state

$$((v_1, \dots, v_n), (f_1, f_2)),$$

where n is the number of corners, by construction each v_i and f_i are numbers from $[0, 2\pi]$, because they are angles in radians. Note that v_i are always in ascending order and correspond to the corners of the cloth in order following the border curve. That is, given the border as a sorted list of vertices, v_1 is the coordinate corresponding to the first corner we find in that list. Some examples of the used order are shown at the bottom right of Fig. 8.

Therefore, we can identify what is the semantic state of cloth by using interval reasoning in the circle. Each fold is an interval and we can identify which of the v_i are inside, and these are the folded corners. In addition, each f_i falls inside an edge of the cloth, that is

$$v_j < f_i < v_{j+1} \text{ for any } i \in 1, 2, j \in 1 \dots n,$$

accounting for the $2\pi - 0$ equivalence. The distances of f_i to the neighbors v_i, v_{i+1} are proportional to the distance of where the fold is on the folded edge of the corresponding corner. Therefore, we can also identify where the fold is on the folded edge.

By simple reasoning we can identify if the cloth is folded in a symmetric half, if the two folded edges are both folded by the same proportion, etc. We cannot identify the shape but we can say how many corners it has. Several examples of the obtained labels are showed in Fig. 8. Note that we obtain these without any learning, by just reasoning on our feature vector, and depending on the desired type of labels we can give more abstract or more informed labels. You can find the code to generate the labels in the accompanying website.

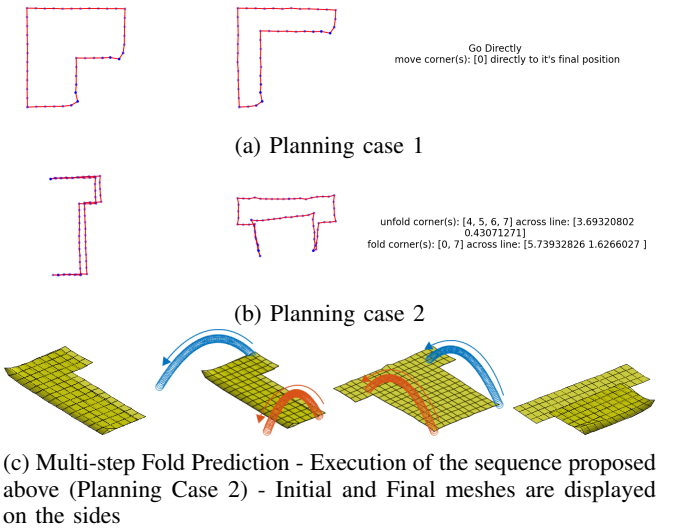


Fig. 9: Planning Outputs

B. Planning

In this section, we show how given the initial border of the cloth, and the CloSE representation of the desired fold state, we can plan a sequence of manipulations and provide the semantic instructions and the low-level trajectory of the corners to manipulate, from the initial position to the end one.

Since the proposed CloSE representation tracks the folds, it can reason over its current state and plan the high-level intermediate states. Fig. 9 shows two representative cases that we encounter when we are dealing with one fold. In case 1, that is, when both the initial and final configurations are in the same semantic region, i.e., the fold encloses the same corner(s), we can directly manipulate the folded corner(s) to their goal position(s), giving both the semantic instruction and the initial and goal positions of the corners we instruct to manipulate, as shown in Fig. 9a.

In case 2, the initial and the goal configurations are in different semantic states, so we might need to take a multi-step approach to reach the goal, whose intermediate state in this case happens to be the unfolded state, as shown in Fig. 9b.

For low-level planning, that is, deciding where to pick the cloth and where to place it, the CloSE representation proves useful. In the cases where there are more than 2 folded corners that require to be moved, we pick 2 corners such that the area of the trapezoid formed between such corners and the fold points on the border is maximum. The idea here is to control the maximum possible area of the cloth. Our manipulation actions are shown in Fig. 9c. We also run the trajectories in simulation to prove the provided instructions can be executed, as can be seen in the video.

VII. CONCLUSION AND FUTURE WORK

In summary, we propose two novel representations for clothes. First, the dGLI disk representation, which extends the work [12] and reveals easy-to-detect geometric shapes

that characterize the cloth state, i.e., how it is folded. Then, we abstract important features from our dGLI representation –the corner and fold locations– and map them onto a circle. This circular representation, which we have named CloSE, is compact and continuous while maintaining the generality for different shapes offered by the dGLI disk. Finally, we show two important applications that come naturally from this representation: Semantic labeling and high- and low-level fold planning.

The current CloSE representation is restricted to single folds; however, the dGLI disk is a very powerful representation and has already shown interesting prospects for coping with multiple folds. Thus, in future work, we plan to extend the functionality of CloSE to handle more complex folding tasks. We have shown in the evaluation that the naive methods used for corner and fold detection in the dGLI disk successfully lead to the desired results through CloSE. Thus, by improving these naive detection methods, CloSE will be enhanced to deal with more complex cloth states.

A good cloth representation is one that allows a robot to reason about cloth states, and plan a sequence of motions to attain a target cloth configuration. Devising a powerful representation for clothes is a very important and difficult problem in robotics and computer graphics. The present work is aimed at being a step in this direction.

REFERENCES

- [1] H. Yin, A. Varava, and D. Kragic, “Modeling, learning, perception, and control methods for deformable object manipulation,” *Science Robotics*, vol. 6, no. 54, p. eabd8803, 2021.
- [2] J. Sanchez, J.-A. Corrales, B.-C. Bouzgarrou, and Y. Mezouar, “Robotic manipulation and sensing of deformable objects in domestic and industrial applications: a survey,” *International Journal of Robotic Research*, vol. 37, no. 7, pp. 688–716, 2018.
- [3] J. Zhu, A. Cherubini, C. Dune, D. Navarro-Alarcon, F. Alambeigi, D. Berenson, F. Ficuciello, K. Harada, J. Kober, X. Li, et al., “Challenges and outlook in robotic manipulation of deformable objects,” *IEEE Robotics & Automation Magazine*, vol. 29, no. 3, pp. 67–77, 2022.
- [4] A. Longhini, Y. Wang, I. Garcia-Camacho, D. Blanco-Mulero, M. Molletta, M. Welle, G. Alenyà, H. Yin, Z. Erickson, D. Held, et al., “Unfolding the literature: A review of robotic cloth manipulation,” *Annual Review of Control, Robotics, and Autonomous Systems*, vol. 8, 2024.
- [5] J. Bednarik, P. Fua, and M. Salzmann, “Learning to reconstruct texture-less deformable surfaces from a single view,” in *Int. Conf. on 3d vision (3DV)*, pp. 606–615, 2018.
- [6] C. Chi and S. Song, “Garmentnets: Category-level pose estimation for garments via canonical space shape completion,” in *Proceedings of the IEEE/CVF International Conference on Computer Vision*, pp. 3324–3333, 2021.
- [7] A. Ramisa, G. Alenyà, F. Moreno-Noguer, and C. Torras, “A 3d descriptor to detect task-oriented grasping points in clothing,” *Pattern Recognition*, vol. 60, pp. 936–948, 2016.
- [8] J. Qian, T. Weng, L. Zhang, B. Okorn, and D. Held, “Cloth region segmentation for robust grasp selection,” in *IEEE/RSJ International Conference on Intelligent Robots and Systems*, pp. 9553–9560, 2020.
- [9] M. Lippi, P. Poklukar, M. C. Welle, A. Varava, H. Yin, A. Marino, and D. Kragic, “Enabling visual action planning for object manipulation through latent space roadmap,” *IEEE Transactions on Robotics*, vol. 39, no. 1, pp. 57–75, 2022.
- [10] D. Tanaka, S. Arnold, and K. Yamazaki, “Emd net: An encode-manipulate-decode network for cloth manipulation,” *IEEE Robotics and Automation Letters*, vol. 3, no. 3, pp. 1771–1778, 2018.
- [11] M. Alberich-Carramiñana, J. Amorós, and F. Coltraro, “Developable surfaces with prescribed boundary,” in *Extended Abstracts GEOMVAP 2019: Geometry, Topology, Algebra, and Applications; Women in Geometry and Topology*, pp. 127–132, Springer, 2021.
- [12] F. Coltraro, J. Fontana, J. Amorós, M. Alberich-Carramiñana, J. Borràs, and C. Torras, “A representation of cloth states based on a derivative of the gauss linking integral,” *Applied Mathematics and Computation*, vol. 457, p. 128165, 2023.
- [13] Z. Huang, X. Lin, and D. Held, “Mesh-based dynamics with occlusion reasoning for cloth manipulation,” in *Robotics: Science and Systems (RSS)*, 2022.
- [14] S. Miller, M. Fritz, T. Darrell, and P. Abbeel, “Parametrized shape models for clothing,” in *IEEE International Conference on Robotics and Automation*, pp. 4861–4868, 2011.
- [15] A. Doumanoglou, J. Stria, G. Peleka, I. Mariolis, V. Petrik, A. Karagakos, L. Wagner, V. Hlavac, T.-K. Kim, and S. Malassiotis, “Folding clothes autonomously: A complete pipeline,” *IEEE Transactions on Robotics*, vol. 32, no. 6, pp. 1461–1478, 2016.
- [16] Y. Li, Y. Yue, D. Xu, E. Grinspun, and P. K. Allen, “Folding deformable objects using predictive simulation and trajectory optimization,” in *IEEE/RSJ Int. Conf. on Intel. Rob. and Sys.*, pp. 6000–6006, 2015.
- [17] R. Hoque, D. Seita, A. Balakrishna, A. Ganapathi, A. K. Tanwani, N. Jamali, K. Yamane, S. Iba, and K. Goldberg, “Visuo-spatial foresight for multi-step, multi-task fabric manipulation,” in *Rob.: Sci. and Sys. (RSS)*, 2020.
- [18] D. Seita, N. Jamali, M. Laskey, A. K. Tanwani, R. Berenstein, P. Baskaran, S. Iba, J. Cann, and K. Goldberg, “Deep transfer learning of pick points on fabric for robot bed-making,” in *International Symposium on Robotics Research (ISRR)*, 2019.
- [19] W. Yan, A. Vangipuram, P. Abbeel, and L. Pinto, “Learning predictive representations for deformable objects using contrastive estimation,” *arXiv preprint arXiv:2003.05436*, 2020.
- [20] V. Ivan, D. Zarubin, M. Toussaint, T. Komura, and S. Vijayakumar, “Topology-based representations for motion planning and generalization in dynamic environments with interactions,” *The International Journal of Robotics Research*, vol. 32, no. 9-10, pp. 1151–1163, 2013.
- [21] D. Zarubin, V. Ivan, M. Toussaint, T. Komura, and S. Vijayakumar, “Hierarchical motion planning in topological representations,” *Proceedings of Robotics: Science and Systems VIII*, 2012.
- [22] F. T. Pokorny, J. A. Stork, and D. Kragic, “Grasping objects with holes: A topological approach,” in *2013 IEEE international conference on robotics and automation*, pp. 1100–1107, IEEE, 2013.
- [23] J. A. Stork, F. T. Pokorny, and D. Kragic, “Integrated motion and clasp planning with virtual linking,” in *2013 IEEE/RSJ International Conference on Intelligent Robots and Systems*, pp. 3007–3014, IEEE, 2013.
- [24] J. A. Stork, F. T. Pokorny, and D. Kragic, “A topology-based object representation for clasping, latching and hooking,” in *2013 13th IEEE-RAS International Conference on Humanoid Robots (Humanoids)*, pp. 138–145, IEEE, 2013.
- [25] W. Yuan, K. Hang, H. Song, D. Kragic, M. Y. Wang, and J. A. Stork, “Reinforcement learning in topology-based representation for human body movement with whole arm manipulation,” in *2019 International Conference on Robotics and Automation (ICRA)*, pp. 2153–2160, IEEE, 2019.
- [26] J. Borràs, A. Boix-Granell, S. Foix, and C. Torras, “A virtual reality framework for fast dataset creation applied to cloth manipulation with automatic semantic labelling,” in *IEEE International Conference on Robotics and Automation (ICRA 2023)*, pp. 0210031–0210311, IEEE, 2023.
- [27] W. Wang, G. Li, M. Zamora, and S. Coros, “Trtm: Template-based reconstruction and target-oriented manipulation of crumpled cloths,” in *2024 IEEE International Conference on Robotics and Automation (ICRA)*, pp. 12522–12528, IEEE, 2024.
- [28] R. Ren, M. Gurnani Rajesh, J. Sanchez-Riera, A. Lopez-Rodriguez, F. Zhang, Y. Tian, G. Alenyà, A. Agudo, Y. Demiris, K. Mikolajczyk, et al., “Grasp-oriented fine-grained cloth segmentation without real supervision,” in *Proceedings of the 2023 6th International Conference on Machine Vision and Applications*, pp. 147–153, 2023.
- [29] S. L. Ho, *Topology-based character motion synthesis*. PhD thesis, University of Edinburgh, 2011.
- [30] M. Ester, H.-P. Kriegel, J. Sander, and X. Xu, “Density-based spatial clustering of applications with noise,” in *Int. Conf. knowledge discovery and data mining*, vol. 240, 1996.
- [31] F. Coltraro, J. Amorós, M. Alberich-Carramiñana, and C. Torras, “A novel collision model for inextensible textiles and its experimental validation,” *Applied Mathematical Modelling*, vol. 128, pp. 287–308, 2024.